Hindawi Publishing Corporation
International Journal of Photoenergy
Volume 2012, Article ID 532843, 10 pages
doi:10.1155/2012/532843

Research Article

Enhancement of Visible-Light Photocatalytic Activity of Mesoporous Au-TiO_2 Nanocomposites by Surface Plasmon Resonance

Minghua Zhou,[1,2] Jun Zhang,[2] Bei Cheng,[2] and Huogen Yu[2]

[1] *Laboratory of Medical Chemistry, Hubei University of Chinese Medicine, Shiyan, Hubei 442000, China*
[2] *State Key Laboratory of Advanced Technology for Material Synthesis and Processing, Materials College, Wuhan University of Technology, 122 Luoshi Road, Wuhan 430070, China*

Correspondence should be addressed to Bei Cheng, chengbei2003@yahoo.com.cn and Huogen Yu, yuhuogen@yahoo.cn

Received 30 October 2011; Accepted 2 November 2011

Academic Editor: Jiaguo Yu

Mesoporous Au-TiO_2 nanocomposite plasmonic photocatalyst with visible-light photoactivity was prepared by a simple spray hydrolytic method using photoreduction technique at 90°C. The prepared samples were characterized by X-ray diffraction, scanning electron microscopy, transmission electron microscopy, and N_2 adsorption-desorption isotherms. The formation of hydroxyl radicals (•OH) on the surface of visible-light illuminated Au-TiO_2 nanocomposites was detected by the luminescence technique using terephthalic acid as probe molecules. The photocatalytic activity was evaluated by photocatalytic decolorization of Rhodamine-B (RhB) aqueous solution under visible-light irradiation ($\lambda > 420$ nm). The results revealed that the TiO_2 could be crystallized *via* spray hydrolysis method, and the photoreduction technique was facilitated to prepare Au nanoparticles in the mesoporous TiO_2 at 90°C. The light absorption, the formation rate of hydroxyl radicals, and photocatalytic decolorization of Rhodamine-B aqueous solution were significantly enhanced by those embedded Au nanoparticles in the Au-TiO_2 nanocomposites. The prepared Au-TiO_2 nanocomposites exhibit a highly visible-light photocatalytic activity for photocatalytic degradation of RhB in water, and their photocatalytic activity is higher than that of the pristine TiO_2 nanoparticles due to the surface plasmon resonance.

1. Introduction

Since the discovery of photocatalytic water splitting on TiO_2 single-crystal electrodes by Fujishima and Honda in 1972 [1], nanosized TiO_2 semiconductor has been always regarded as one of the most promising photocatalysts in practical applications, especially water cleaning and removal of volatile organic compounds (VOCs) in air, due to its high photocatalytic activity, chemical stability, low cost, and nontoxicity [2–12]. Recently, highly dispersed noble metal nanoparticles with desirable morphologies have attracted great attention due to their unusual catalytic, electric, optical properties and surface plasmon absorption, and their widespread potential usefulness in diverse fields such as biomedicine, photocatalysis, energy conversion, and storage and nanodevices [13–19]. Some investigations have indicated that nobel metal Au nanoparticles deposited on TiO_2 surface can obviously enhance the photocatalytic performance *via* suppressing the recombination of electron-hole pairs, and also extending the light response in the visible region [14, 20, 21]. However, the practical applicability of such a composite structure is limited owing to exposing both the Au nanoparticles to reactants and the surrounding, while the corrosion or dissolution of the Au nanoparticles during the photocatalytic reaction is likely to limit the usage of Au, especially for long-term working [13]. To overcome this shortcoming, the Au nanoparticles embeded or enwrapped by the TiO_2 aggregates have attracted considerable attention, and significant advances have been made in recent years. The TiO_2 aggregates offer protection for Au nanoparticles against dissolution, photocorrosion, and chemical corrosion under extreme conditions, as well as being used for decomposition of dye wastewater. Among the various phases of TiO_2, anatase has proven to be the most suitable one due to its

two distinctive performances. One is that the photogenerated electrons of anatase can rapidly reduce Au ions at interface [22]. The other is that the conduction band of anatase can transfer the photogenerated electrons of the excited Au to adsorbed O_2 and then to form active superoxide radical anions [23–25].

Several techniques, such as sol-gel method, chemical vapor deposition, laser vaporization, modified impregnation, precipitation-reduction, and photoreduction, have been developed to design and modulate the Au-TiO_2 composite nanoparticles. The preferred and versatile method is the sol-gel process, which has many advantages, such as simple equipment required, flexible control of pore structures, and the concentration of Au [26–30]. Usually, the TiO_2 aggregates obtained by this method are amorphous in nature and calcination temperatures higher than 400°C are required to realize the phase transformation from amorphous to anatase. However, such high calcination temperatures will not only lead to the increase of crystallite size and the decrease of specific surface areas and pore volume, but also induce the heat-aggregation of Au nanoparticles. Generally, the Au particles have exhibited highly catalytic activity only with smaller nanoscale size [31–34]. So, in order to obtain crystallized Au-TiO_2 composite nanoparticles with higher specific surface areas and pore volume, the temperature of phase transformation from amorphous to anatase must be lowered.

In this paper, a novel and simple method, a low-temperature spray hydrolysis assisted with photoreduction tech nique, was proposed for the synthesis of Au-TiO_2 nanocomposites. The Au nanoparticles (Au colloids) were prepared by photoreduction technique using a 350 W xenon lamp as a light source. Au-TiO_2 nanocomposites were prepared by spraying the mixed solution of $Ti(OC_4H_9)_4$ and EtOH into hot distilled water in the presence of Au nanoparticles (ca. 90°C). The formation of hydroxyl radicals (•OH) on the surface of visible-light illuminated Au-TiO_2 composite samples was detected by the photoluminescence technique using terephthalic acid as probe molecules. The photocatalytic activity of the Au-TiO_2 composite samples was evaluated by photocatalytic decolorization of RhB aqueous solution under visible-light irradiation ($\lambda > 420$ nm).

2. Experimental

2.1. Preparation of Au Nanoparticles. All the involved chemicals in this study were purchased from Shanghai Chemical Reagent Co., Ltd, and used without further purification. Typically, 10 mL aqueous solution of sodium citrate (38.8 mM) was added into 100 mL aqueous solution of $HAuCl_4 \cdot 4H_2O$ (1 mM) under vigorous stirring. A 350 W xenon lamp was used a light source to irradiate the mixed solution during the reduction process. The color of the solution was gradually changed from light-yellow to fuchsia. After irradiation for another 30 mins, it was cooled to room temperature.

2.2. Preparation of Au-TiO_2 Composite Nanoparticles. In a typical synthesis [35], 10 mL of mixed solution of Tetrabutyl titanate (TBOT) and ethanol (volume ratio of TBOT to ethanol, 1 : 4) was sprayed into a 250 mL beaker containing 200 mL hot distilled water (90°C), in which the added above Au nanoparticles was used as Au source. The corresponding nominal atomic ratio of Au to Ti, which hereafter was designated as R_{Au}, was 0.003, 0.006, 0.015, 0.030, and 0.060 nominal atomic % (at. %). After further stirring for 2 h at 90°C, the resultant mixed solution was aged for 2 h at 90°C. The aged wet precipitates were filtrated, rinsed with distilled water and absolute alcohol for two times. Then the precipitates were dried in a vacuum oven at 80°C for 10 h and finally ground to obtain Au-TiO_2 composite samples. As a control experiment, the pristine TiO_2 product was also prepared under the same condition but without adding Au nanoparticles.

2.3. Characterization. X-ray diffraction (XRD) patterns obtained on a D/Max-RB X-ray diffractometer (Rigaku, Japan) using Cu Kα irradiation at a scan rate (2θ) of 0.05° s^{-1} were used to determine the phase structure of the obtained samples. The average crystallite sizes of anatase were determined according to the Scherrer equation using the full width at half maximum (FWHM) data of anatase phase after correcting the instrumental broadening. Morphology observation was performed on a S-4800 field emission scanning electron microscope (FESEM, Hitachi, Japan). Transmission electron microscopy (TEM) and high-resolution transmission electron microscopy (HRTEM) observation were conducted using a JEM 2100F microscope at an accelerating voltage of 200 kV. The Brunauer-Emmett-Teller surface areas (S_{BET}) of the samples were analyzed by nitrogen adsorption in a Micromeritics ASAP 2020 nitrogen adsorption apparatus (USA). All the samples were degassed at 80°C prior to nitrogen adsorption measurements. The BET surface area was determined by a multipoint BET method using the adsorption data in the relative pressure (P/P_0) range of 0.05 to 0.30. Desorption isotherm was used to determine the pore size distribution via the Barret-Joyner-Halender (BJH) method, assuming a cylindrical pore modal [36]. The nitrogen adsorption volume at the relative pressure (P/P_0) of 0.994 was used to determine the pore volume and average pore size. UV-visible absorbance spectra of Au-TiO_2 composite nanoparticles were obtained for the dry-pressed disk samples with a UV-visible spectrophotometer (UV-2550, Shimadzu, Japan). $BaSO_4$ was used as a absorption standard in the UV-visible absorbance experiment. X-ray photoelectron spectroscopy (XPS) measurements were performed on a Kratos XSAM800 XPS system with Cu Kα source. During the experiments the pressure in the chambers was about 10^{-7} Pa. All the binding energies were referenced to the C1s peak at 284.8 eV of the surface adventitious carbon.

2.4. Analysis of Hydroxyl Radical (•OH). The formation of hydroxyl radical (•OH) on the surface of photoirradiated Au-TiO_2 is detected by photoluminescence (PL) technique using terephthalic acid as a probe molecule. Terephthalic acid readily reacts with •OH to produce highly fluorescent product, 2-hydroxyterephthalic acid [37, 38]. This technique has

been widely used in radiation chemistry, sonochemistry, and biochemistry [37–39] for the detection of •OH generated in water. The intensity of the PL peak of 2-hydroxyterephtalic acid is in proportional to the amount of •OH radicals produced in water [37–39]. The optimal concentration of terephthalic acid solution was about 5×10^{-4} M in a diluted NaOH aqueous solution (2×10^{-3} M). This method relies on the PL signal at 425 nm of the hydroxylation of terephthalic acid with •OH generated at the water/TiO_2 interface. The method is rapid, sensitive, and specific, only needs a simple standard PL instrumentation.

In order to measure the concentration of hydroxyl radical (•OH) of the prepared samples, the typical experimental procedures are as follows Au-TiO_2 composite samples were weighed and then uniformly dispersed into 20 mL distilled water under 10 min ultrasonic shaking to form TiO_2 suspension. The photocatalyst was prepared by coating the above aqueous suspension of TiO_2 samples onto one dish with a diameter of about 9.0 cm. The weight of catalysts used for each experiment was kept 0.10 g. The dishes containing composite powders were dried in an oven at 80°C for about 2 h to evaporate the water and then cooled to room temperature before being used. A 20 mL of the 5×10^{-4} M terephthalic acid aqueous solution with a concentration of 2×10^{-3} M NaOH was added into the coated dish, which was then irradiated with a 15 W daylight lamp. In order to ensure only the visible light irradiation, each dish was covered with an ultraviolet cutoff filter ($\lambda > 420$ nm). PL spectra of generated 2-hydroxyterephthalic acid were measured on a fluorescence spectrophotometer (F-7000, Hitachi, Japan) using a 315 nm excitation wavelength at a scan speed of 1200 nm min^{-1} with the PMT voltage of 700 V. The width of excitation slit and emission slit were 1.0 nm.

2.5. Photocatalytic Activity. The visible-light photocatalytic activity of the Au-TiO_2 composite samples was evaluated by photocatalytic decolorization of RhB aqueous solution. The detailed procedure was similar to our previous works [40]. Here, the weight of the photocatalyst used was kept at about 0.1 g. A 15 W daylight lamp (6 cm above the dishes, just mentioned above) was used as a light source and each dish was covered with an ultraviolet cutoff filter. The absorbance of RhB was determined by a UV-visible spectrophotometer (UV2550, Shimadzu, Japan). The concentration of RhB (c) was in proportion to the light absorbance (A) at 550 nm according to Beer-Lambert law. As for the Rhodamine-B aqueous with a concentration of 1×10^{-5} M, its photocatalytic decolorization is a pseudofirst-order reaction and its kinetics may be expressed as [41, 42]:

$$\ln \frac{A_0}{A_t} = kt, \quad (1)$$

where k is the apparent rate constant, and A_0 and A_t are the initial and reaction absorbance of RhB aqueous, respectively.

3. Results and Discussion

3.1. Phase Structures. XRD was used to investigate the changes of phase structure of the as-prepared Au-TiO_2 nanocomposites and pure TiO_2. Figure 1 shows the effects of R_{Au} on phase structures of the Au-TiO_2 composite powders. It can be seen that the diffraction peaks of all samples were indexed with the anatase phase of TiO_2, which was consistent with our previous work [35]. With increasing the R_{Au}, the intensities of anatase peaks steadily become weaker and the width of the diffraction peaks ($2\theta = 25.3°$) of anatase slightly became wider. This was probably due to the fact that Au nanoparticles suppress the crystallization of TiO_2 xerogel powders. However, the XRD diffraction peaks of Au could not be seen in the Figure 1, which was attributed to the fact that the content of Au was so low that it could not be detected by XRD diffractometer.

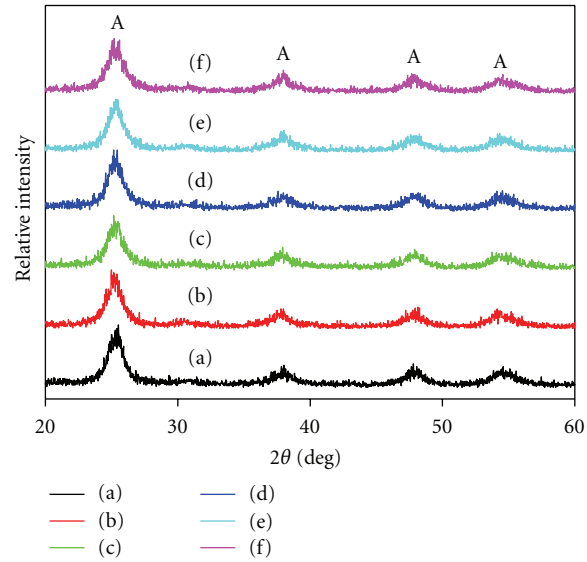

FIGURE 1: XRD patterns of the Au-TiO_2 composite powders prepared with different R_{Au}: (a) 0, (b) 0.003, (c) 0.006, (d) 0.015, (e) 0.030, and (f) 0.060.

The microstructure of the Au-TiO_2 composite powder was further studied by TEM and HRTEM. Figure 2(a) shows the TEM image of the R_{Au}-0.060 composite sample. It can be observed from Figure 2(a) that the nanocrystallite appears as an agglomerated status, and mesoporous structures without a long-range order. The size of the primary particles estimated from the TEM image was about 6 ± 1 nm, which was in accord with the value of crystallize size (6.0 nm) calculated from XRD pattern using the Scherrer equation (as shown in Table 1). Figure 2(b) shows the corresponding HRTEM image of the R_{Au}-0.060 composite powder. Further observation shows that all the particles are crystallized as evidence from the well-resolved Au (111) (0.25 nm) and TiO_2 (101) (0.35 nm) crystalline lattices as shown in the inset of Figure 2(b) [42–44].

Effects of the R_{Au} on the surface morphology of the prepared Au-TiO_2 composite powders were characterized by FESEM. Figure 3 illustrates FESEM images of all the Au-TiO_2 composite powders, indicating their nonuniform growth and particle size distribution in spherical morphology, which changed slightly with the different Au modification. This agglomeration process was attributed to Van der Waals

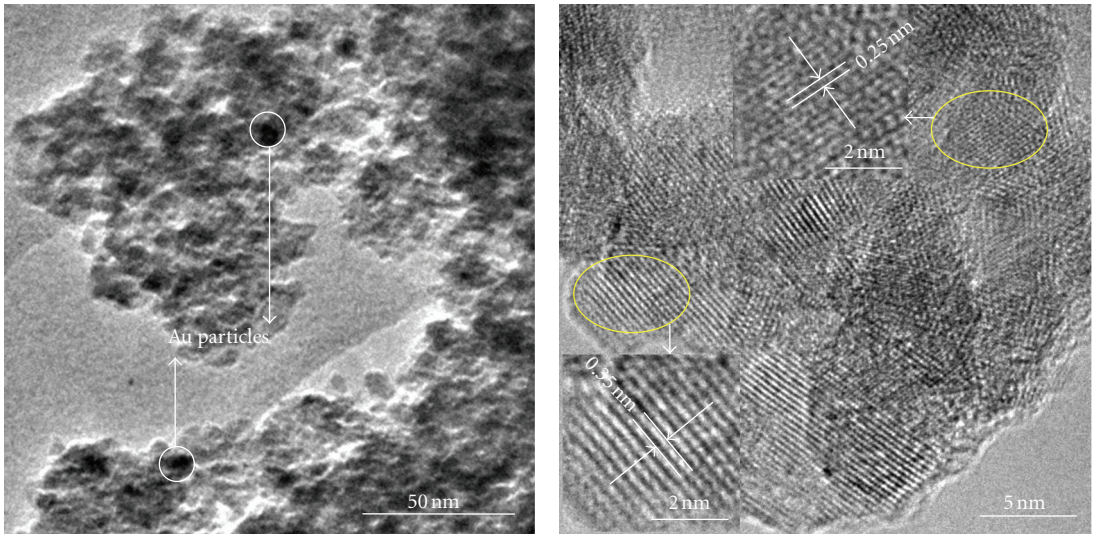

(a) (b)

Figure 2: TEM (a) and HRTEM (b) images of the R_{Au}-0.060 composite powder.

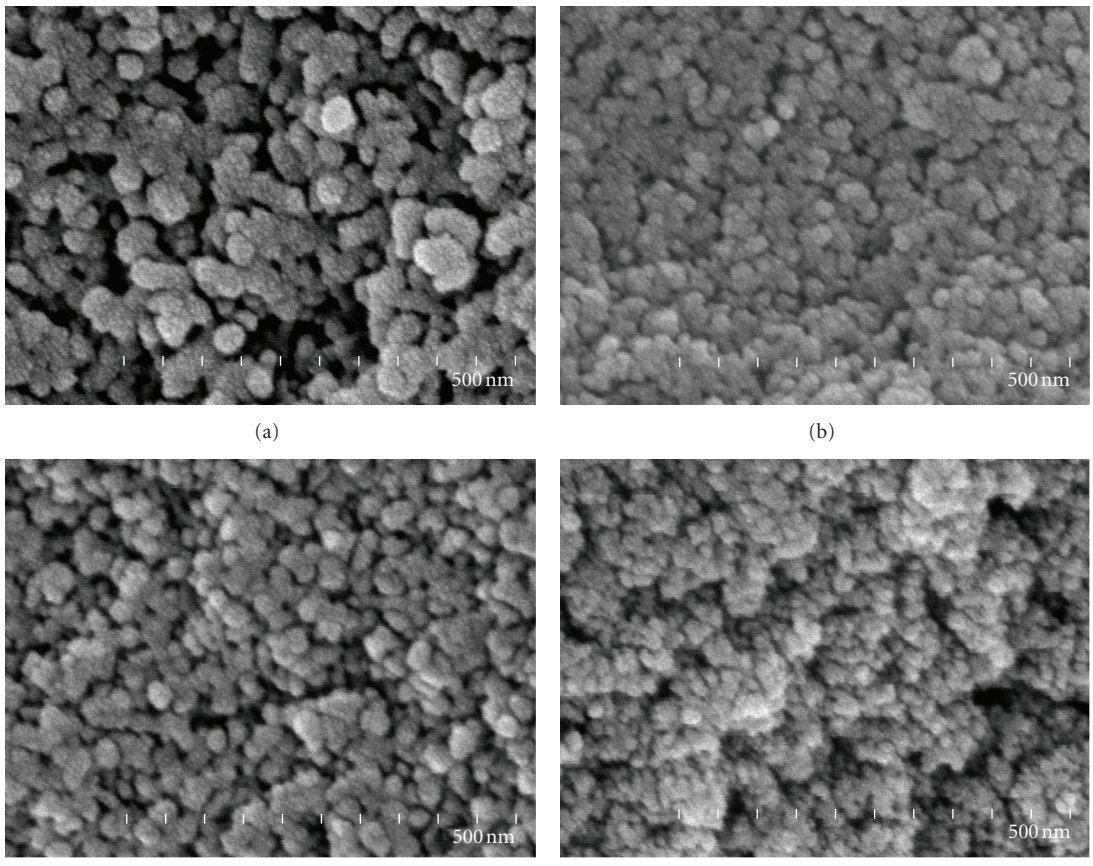

(a) (b)

(c) (d)

Figure 3: FESEM images of the Au-TiO_2 composite powders prepared with different R_{Au}: (a) 0, (b) 0.003, (c) 0.015, and (d) 0.060.

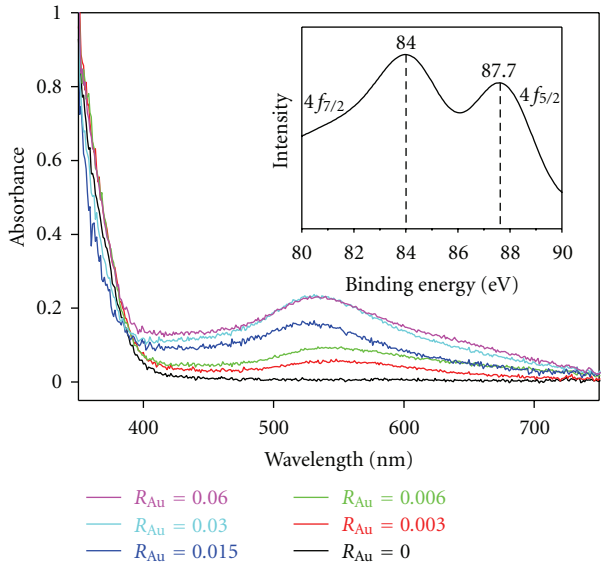

FIGURE 4: UV-Vis absorbance spectra of the Au-TiO_2 composite powders prepared with different R_{Au} and (inset) high-resolution XPS spectrum of Au 4f of the R_{Au}-0.060 sample.

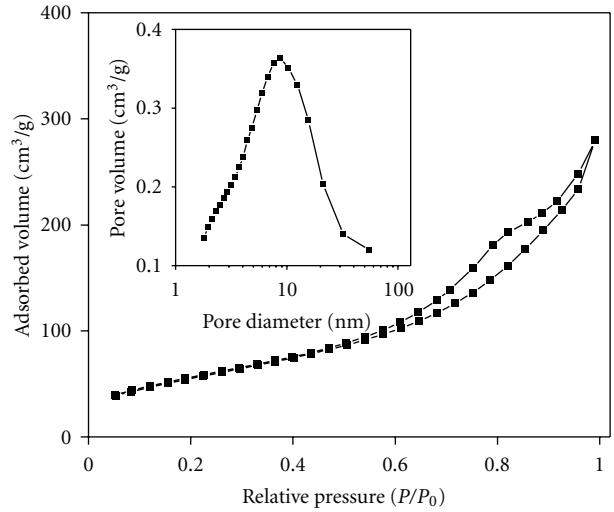

FIGURE 5: N_2 adsorption-desorption isotherm and pore size distribution curve (inset) of the R_{Au}-0.015 composite powder.

forces. In order to reduce the surface energy, the primary particles have a tendency to form an agglomerate, by forming nearly spherical or equiaxed agglomerates, in a minimum surface-to-volume ratio and hence minimum surface free energy can be achieved. All the Au-TiO_2 composite powders are composed of such nanoscale particles, indicating that the composite powders prepared by this low-temperature spray method possess large specific surface area and the high volume fraction of atoms located both on the surface and at the grain boundaries. Therefore, this Au-TiO_2 composite nanocrystalline can provide more active sites for catalysis. Furthermore, all the Au-TiO_2 composite powders have roughness surface accompanied with many mesopores. In general, such nanoscale particles with such diameter will be more promising because light harvesting can be further enhanced. In this respect, nanocrystalline Au-TiO_2 composite particles with this special morphology can enhance the absorbance of the light resulting in the enhancement of photocatalytic activity. Further observations indicated that the powders without Au nanoparticles modification (pristine TiO_2) have large particles. With increasing the R_{Au}, the average size of aggregated particles decreases.

3.2. UV-Visible Absorbance Spectra. Figure 4 shows UV-Vis absorbance spectra for the composite Au-TiO_2 samples. A significant increase at wavelengths longer than 400 nm could be attributed to the plasmon resonance absorbance of the Au nanoparticles [22, 44]. The Au-TiO_2 composite powders compared with the pristine TiO_2 powders have a slight red shift in the band gap transition. Moreover, a characteristic absorbance signal at 530 nm give the valid evidence that the Au phase existed in the products, though direct observation by XRD failed [24, 33, 45–47]. Further observation indicates that the intensity of the surface plasmon absorbance increase with increasing R_{Au}, which is probably due to the more Au nanoparticles embeded in TiO_2 aggregates. The enhanced light absorption in the visible light region can therefore increase the quantities of photogenerated electrons and holes that participate in photocatalytic reactions. In order to verify the chemical state of Au element in the Au-TiO_2 composite powders, the R_{Au}-0.060 sample was also characterized with XPS. High-resolution XPS spectrum (inset in Figure 4) shows binding energy of $Au_{4f7/2}$ at 84.0 and $Au_{4f5/2}$ at 87.7 eV, which are significantly different from $Au^{+}_{4f7/2}$ (84.6 eV) and $Au^{3+}_{4f7/2}$ (87.0 eV). The result suggests that the Au species is in the metallic state [25, 44, 48, 49].

3.3. BET Specific Surface Areas and Pore Structure. All the prepared Au-TiO_2 composite powders have similar nitrogen adsorption-desorption isotherms and pore size distribution curves. Therefore, Figure 5 only presents the nitrogen adsorption-desorption isotherm and pore size distribution (inset) of the R_{Au}-0.015 sample. It can be seen that isotherm was of types IV [36]. At high relative pressure range from 0.5 to 1.0, the isotherm exhibits a hysteresis loop of type H2 associated with the ink bottle pores, indicating that the powders contain mesopores due to the aggregation of crystallites [4–6]. The corresponding pore size distribution curve of the R_{Au}-0.015 sample is also shown in inset of Figure 5. It can be seen that the R_{Au}-0.015 sample exhibits a narrow pore size distribution with the average pore diameters about 5.7 nm.

Table 1 shows the effects of R_{Au} on the physical properties of the Au-TiO_2 composite powders. It can be seen that all the prepared samples possess large specific surface area (S_{BET} > 200 m^2/g) and big pore volume (V_p > 0.30 cm^3/g). With increasing R_{Au}, the average pore sizes decrease from 8.1 to 5.4 nm while the specific surface area and pore volume change slightly. Generally, the heterogeneous photocatalysis is a surface-based process, and therefore a large surface area has positive effects on such a process. A larger surface

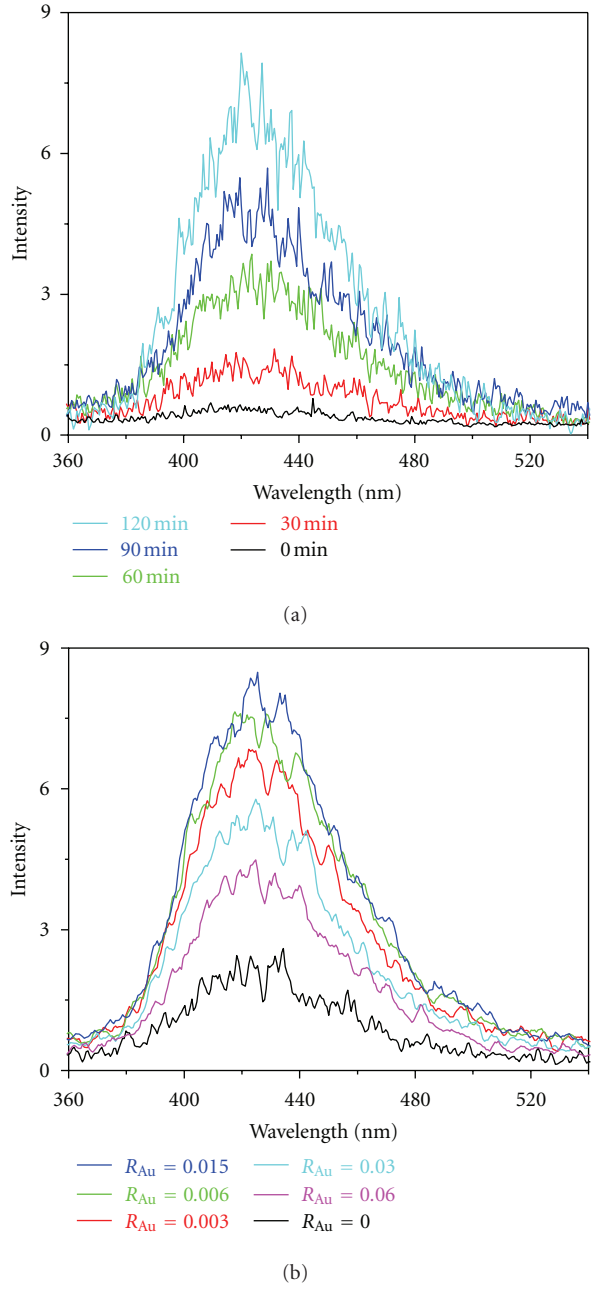

FIGURE 6: (a) Fluorescence spectral changes with irradiation time on R_{Au}-0.015 sample and (b) the dependence of the fluorescence intensity on R_{Au} at a fixed 120 min under visible-light irradiation.

area provides more surface active sites for the adsorption of reactant molecules, which thus make the photocatalytic process more efficient [50–53]. Moreover, the porous structure is believed to facilitate the transporting of reactant molecules and products through the interior space due to the interconnected porous networks, and it favor the harvesting of exciting light due to enlarged surface area and multiple scattering within the porous framework [54–56].

3.4. Hydroxyl Radical Analysis. The PL emission spectrum excited at 315 nm of terephthalic acid solution was measured

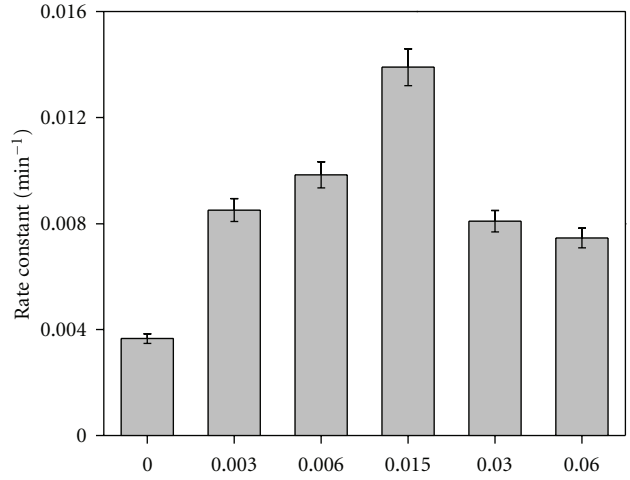

FIGURE 7: Dependence of apparent rate constants (k) of the Au-TiO_2 composite samples on the R_{Au}.

every 30 min under visible-light irradiation. Figure 6(a) shows the changes of PL spectra of terephthalic acid solution with irradiation time. It can be seen that a gradual increase in PL intensity at wavelength range of 360–540 nm is observed with increasing irradiation time. Moreover, the generated spectra have the identical shape and peak position (at 425 nm). However, no PL increase is observed in the absence of visible-light or TiO_2 samples. This suggests that the signal of PL is only caused by the reaction of terephthalic acid with •OH formed on the interface of the Au-TiO_2/water during visible-light irradiation [37, 38].

Generally, the greater the formation rate of •OH radicals is, the higher separation efficiency of electron-hole pairs is achieved. So, the photocatalytic activity is in positive correlation to the formation rate of •OH radicals, namely, a faster formation rate of •OH radicals leads to a higher photocatalytic activity [38]. Figure 6(b) shows the dependence of PL intensity against irradiation time. It can be easily seen that at a fixed time (120 min), the formation rate of •OH radicals on the Au-TiO_2 composite powders is larger than that of the pristine TiO_2. This implies that the Au-TiO_2 composite powders have higher photocatalytic activity than the pristine TiO_2. Further observation shows that the order of the formation rate of •OH radicals formed on the surface of as-prepared samples is as follows: R_{Au}-0.015 > R_{Au}-0.006 > R_{Au}-0.003 > R_{Au}-0.030 > R_{Au}-0.060 > R_{Au}-0 (pristine TiO_2), which suggests that the R_{Au} influences the formation rate of •OH radicals and there is an optimum ratio of Au to TiO_2.

3.5. Photocatalytic Activity of the Au-TiO_2 Composite Powders. The photocatalytic activity of the Au-TiO_2 composite powders was evaluated by photocatalytic decolorization of Rhodamine-B aqueous solution under visible-light irradiation (λ > 420 nm) at room temperature. Figure 7 shows the relationship between the apparent rate constants (k) and R_{Au}. It can be seen that the R_{Au} has a great effect on the photocatalytic activity of the composite samples. Without

Table 1: Effects of R_{Au} on physical properties of the Au-TiO_2 composite powders.

Sample (R_{Au})	Phase content	[a]Crystalline size/nm	[b]S_{BET} m^2/g	[c]V_p cm^3/g	[c]Porosity (%)	[c]Average pore size/nm
0	Anatase	6.7	235.5	0.57	69.0	8.1
0.003	Anatase	6.7	208.4	0.46	64.2	7.5
0.006	Anatase	6.5	211.7	0.34	57.0	7.1
0.015	Anatase	6.5	205.0	0.43	62.6	5.7
0.030	Anatase	6.3	215.9	0.38	59.7	5.8
0.060	Anatase	6.0	212.4	0.34	57.0	5.4

[a]: Average crystalline size of TiO_2 was determined on the basis of the broadening of the anatase {101} diffraction peak using the Scherrer equation.
[b]: The BET surface area was determined by multipoint BET method using the adsorption data in the relative pressure (P/P_0) range of 0.05–0.2.
[c]: Pore volume, porosity, and average pore size were determined by nitrogen adsorption volume at the relative pressure of 0.994.

Au modification, the prepared pristine TiO_2 powders have the poor visible-light photocatalytic activity presumably due to the self-sensitization of RhB molecules, which extends the absorption of titania into the visible-light region [57]. Importantly, the photocatalytic activity of all Au-TiO_2 samples is higher than that of pristine TiO_2. Further observation shows the reaction rate increases with the increasing of Au content when the value of R_{Au} is below 0.015, and the R_{Au}-0.015 sample has the best photocatalytic activity among these samples. Therefore, the appropriate modification of the gold nanoparticles can enhance the photocatalytic activity of TiO_2 remarkably, which is ascribed to the synergetic effect of the dye-photosensitized and the surface plasmon resonance of Au nanoparticles in the Au-TiO_2 nanocomposites.

The possible photocatalytic enhanced mechanism of the Au-TiO_2 nanocomposite powders can be explained according to the recently reported mechanism [4, 15, 22, 47]. The noble metal nanoparticles can be photoexcited by the visible light due to their plasmon resonance. Under visible-light irradiation, the electrons and holes can be formed on the surface of the Au nanoparticles, and then they are immediately separated via the following processes. The electrons transfer to the adsorbed oxygen molecules via the conduction band of TiO_2 and then are trapped through formation of superoxide radical anions. The superoxide radicals and the trapped electrons can combine to produce H_2O_2, finally forming hydroxyl radicals. Both hydroxyl radical and superoxide radical anions are strong oxidants which can oxidize the organic molecules (RhB) on the surface of the composite powders, resulting in the formation of intermediate organic species and subsequently complete oxidation of these species to water and carbon dioxide. These improvements would be beneficial to the photooxidation of RhB using the Au modified TiO_2 under visible-light irradiation. When the R_{Au} reaches 0.030, the Au-TiO_2 composite powders show relatively lower photocatalytic activity, which is probably due to the fact that more Au nanoparticles may act as the centers of electron-hole recombination and reduce quantum efficiency [44].

Figure 8 shows the change of absorption spectra of RhB aqueous solution during its visible-light photocatalytic decolorization using the R_{Au}-0.015 sample as the photocatalyst. It can be seen that the absorption peak at $\lambda = 550$ nm drops gradually with increasing visible-light irradiation time. After visible-light irradiation for ca. 180 minutes, the absorption peak of RhB aqueous solution is very weak and the color of the RhB aqueous solution changes from orange to near no color, indicating that the Au-TiO_2 composite powders can completely decolorize RhB aqueous solution under visible-light irradiation. Usually, the complete decolorization of RhB requires a long time due to the fact that its decolorization goes through two different stages: the ring cleavage in the initial photocatalytic degradation stage and subsequent oxidation of the fragments in the latter stage [40, 58]. Therefore, these composite powders prepared by this method could be useful for environmental applications such as air purification, water disinfection and purification, and hazardous waste remediation due to their cheap preparation process, controllable structure, large specific surface area, and high visible-light photocatalytic activity.

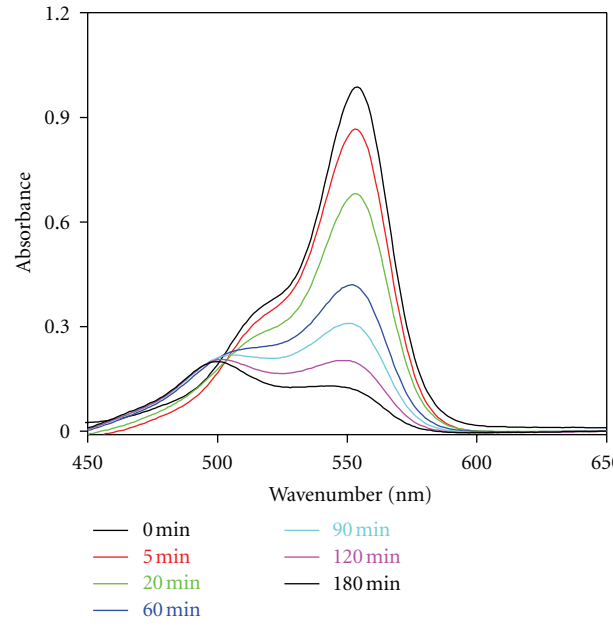

Figure 8: The dependence of absorbance (A) of RhB aqueous solution on the visible-light irradiation time.

4. Conclusions

Au-TiO_2 nanocomposites can be facilely prepared by a simple spray hydrolytic method and assisted with photoreduction technique at 90°C. The light absorption, the

formation rates of hydroxyl radicals, and photocatalytic decolorization of RhB aqueous solution were significantly enhanced by those embeded Au nanoparticles in the Au-TiO_2 nanocomposites due to surface plasmon resonance of Au nanoparticles. The composite R_{Au}-0.015 sample exhibited the best visible-light photocatalytic activity for photocatalytic decolorization of RhB aqueous solution due to the synergistic effects of the absorption shift into visible and improved efficiency of interfacial charge transfer process.

Acknowledgments

This paper was partially supported by the National Natural Science Foundation of China (51072154 and 51102190), Natural Science Foundation of Hubei Province (2010CDA078), National Basic Research Program of China (2009CB939704), and Self-determined and Innovative Research Funds of SKLWUT. This paper was also supported by the Key Science Research Project of the Hubei Provincial Department of Education (D20112107) and the Science Research Project of Hubei University of Medicine (2009QDJ25).

References

[1] A. Fujishima and K. Honda, "Electrochemical photolysis of water at a semiconductor electrode," *Nature*, vol. 238, no. 5358, pp. 37–38, 1972.

[2] M. A. Fox and M. T. Dulay, "Heterogeneous photocatalysis," *Chemical Reviews*, vol. 93, no. 1, pp. 341–357, 1993.

[3] M. R. Hoffmann, S. T. Martin, W. Choi, and D. W. Bahnemann, "Environmental applications of semiconductor photocatalysis," *Chemical Reviews*, vol. 95, no. 1, pp. 69–96, 1995.

[4] J. Zhou, Y. Cheng, and J. Yu, "Preparation and characterization of visible-light-driven plasmonic photocatalyst Ag/AgCl/TiO_2 nanocomposite thin films," *Journal of Photochemistry and Photobiology A*, vol. 223, no. 2-3, pp. 82–87, 2011.

[5] J. Yu, T. Ma, and S. Liu, "Enhanced photocatalytic activity of mesoporous TiO_2 aggregates by embedding carbon nanotubes as electron-transfer channel," *Physical Chemistry Chemical Physics*, vol. 13, no. 8, pp. 3491–3501, 2011.

[6] J. Yu, Y. Su, and B. Cheng, "Template-free fabrication and enhanced photocatalytic activity of hierarchical macro-/mesoporous titania," *Advanced Functional Materials*, vol. 17, no. 12, pp. 1984–1990, 2007.

[7] S. Wang, L. Zhao, J. Ran, Z. Shu, G. Dai, and P. Zhai, "Effects of calcination temperatures on photocatalytic activity of ordered titanate nanoribbon/SnO_2 films fabricated during an EPD process," *International Journal of Photoenergy*, vol. 2012, Article ID 472958, 7 pages, 2012.

[8] H. Fu, G. Shang, S. Yang, and T. Xu, "Mechanistic study of visible-light-induced photodegradation of 4-chlorophenol by $TiO_{2-X}N_X$ ($0.021 < x < 0.049$) with low nitrogen concentration," *International Journal of Photoenergy*, vol. 2012, Article ID 759306, 9 pages, 2012.

[9] S.-J. Kim, N.-H. Lee, H.-J. Oh, S.-C. Jung, W.-J. Lee, and D.-H. Kim, "Photocatalytic properties of nanotubular-shaped TiO_2 powders with anatase phase obtained from titanate nanotube powder through various thermal treatments," *International Journal of Photoenergy*, vol. 2011, Article ID 327821, 7 pages, 2011.

[10] J. A. Byrne, P. A. Fernandez-Ibañez, P. S. M. Dunlop, D. M. A. Alrousan, and J. W. J. Hamilton, "Photocatalytic enhancement for solar disinfection of water: a review," *International Journal of Photoenergy*, vol. 2011, Article ID 798051, 12 pages, 2011.

[11] W.-C. Oh and M.-L. Chen, "The improved photocatalytic properties of methylene blue for V_2O_3/CNT/TiO_2 composite under visible light," *International Journal of Photoenergy*, vol. 2010, Article ID 264831, 5 pages, 2010.

[12] Z. Zhang and J. Gamage, "Applications of photocatalytic disinfection," *International Journal of Photoenergy*, vol. 2010, Article ID 764870, 11 pages, 2010.

[13] T. Hirakawa and P. V. Kamat, "Charge separation and catalytic activity of Ag@TiO_2 core-shell composite clusters under UV-irradiation," *Journal of the American Chemical Society*, vol. 127, no. 11, pp. 3928–3934, 2005.

[14] P. Mulvaney, "Surface plasmon spectroscopy of nanosized metal particles," *Langmuir*, vol. 12, no. 3, pp. 788–800, 1996.

[15] Q. Xiang, J. Yu, B. Cheng, and H. C. Ong, "Microwave-hydrothermal preparation and visible-light photoactivity of plasmonic photocatalyst Ag-TiO_2 nanocomposite hollow spheres," *Chemistry—An Asian Journal*, vol. 5, no. 6, pp. 1466–1474, 2010.

[16] B. Cheng, Y. Le, and J. Yu, "Preparation and enhanced photocatalytic activity of Ag@TiO_2 core-shell nanocomposite nanowires," *Journal of Hazardous Materials*, vol. 177, no. 1–3, pp. 971–977, 2010.

[17] J. J. Mock, M. Barbic, D. R. Smith, D. A. Schultz, and S. Schultz, "Shape effects in plasmon resonance of individual colloidal silver nanoparticles," *Journal of Chemical Physics*, vol. 116, no. 15, pp. 6755–6759, 2002.

[18] R. Jin, Y. C. Cao, E. Hao, G. S. Métraux, G. C. Schatz, and C. A. Mirkin, "Controlling anisotropic nanoparticle growth through plasmon excitation," *Nature*, vol. 425, no. 6957, pp. 487–490, 2003.

[19] F. Kim, J. H. Song, and P. Yang, "Photochemical synthesis of gold nanorods," *Journal of the American Chemical Society*, vol. 124, no. 48, pp. 14316–14317, 2002.

[20] M. Jakob, H. Levanon, and P. V. Kamat, "Charge distribution between UV-irradiated TiO_2 and gold nanoparticles: determination of shift in the Fermi level," *Nano Letters*, vol. 3, no. 3, pp. 353–358, 2003.

[21] V. Subramanian, E. E. Wolf, and P. V. Kamat, "Catalysis with TiO_2/gold nanocomposites. Effect of metal particle size on the fermi level equilibration," *Journal of the American Chemical Society*, vol. 126, no. 15, pp. 4943–4950, 2004.

[22] Y. Tian and T. Tatsuma, "Mechanisms and applications of plasmon-induced charge separation at TiO_2 films loaded with gold nanoparticles," *Journal of the American Chemical Society*, vol. 127, no. 20, pp. 7632–7637, 2005.

[23] L. Xiao, J. Zhang, Y. Cong, B. Tian, F. Chen, and M. Anpo, "Synergistic effects of doped Fe(3+) and deposited Au on improving the photocatalytic activity of TiO_2," *Catalysis Letters*, vol. 111, no. 3-4, pp. 207–211, 2006.

[24] R. S. Sonawane and M. K. Dongare, "Sol-gel synthesis of Au/TiO_2 thin films for photocatalytic degradation of phenol in sunlight," *Journal of Molecular Catalysis A*, vol. 243, no. 1, pp. 68–76, 2006.

[25] V. Iliev, D. Tomova, L. Bilyarska, and G. Tyuliev, "Influence of the size of gold nanoparticles deposited on TiO_2 upon the photocatalytic destruction of oxalic acid," *Journal of Molecular Catalysis A*, vol. 263, no. 1-2, pp. 32–38, 2007.

[26] F. B. Li, X. Z. Li, and M. F. Hou, "Photocatalytic degradation of 2-mercaptobenzothiazole in aqueous La^{3+}-TiO_2 suspension

for odor control," *Applied Catalysis B*, vol. 48, no. 3, pp. 185–194, 2004.

[27] D. I. Enache, J. K. Edwards, P. Landon et al., "Solvent-free oxidation of primary alcohols to aldehydes using Au-Pd/TiO_2 catalyst," *Science*, vol. 311, no. 5759, pp. 362–365, 2006.

[28] F. Boccuzzi, A. Chiorino, M. Manzoli et al., "Au/TiO_2 nanosized samples: a catalytic, TEM, and FTIR study of the effect of calcination temperature on the CO oxidation," *Journal of Catalysis*, vol. 202, no. 2, pp. 256–267, 2001.

[29] M. Daté and M. Haruta, "Moisture effect on CO oxidation over Au/TiO_2 catalyst," *Journal of Catalysis*, vol. 201, no. 2, pp. 221–224, 2001.

[30] X. Z. Li and F. B. Li, "Study of Au/Au^{3+}-TiO_2 photocatalysts toward visible photooxidation for water and wastewater treatment," *Environmental Science and Technology*, vol. 35, no. 11, pp. 2381–2387, 2001.

[31] N. Lopez, J. K. Nørskov, T. V. W. Janssens et al., "The adhesion and shape of nanosized Au particles in a Au/TiO_2 catalyst," *Journal of Catalysis*, vol. 225, no. 1, pp. 86–94, 2004.

[32] I. M. Arabatzis, T. Stergiopoulos, D. Andreeva, S. Kitova, S. G. Neophytides, and P. Falaras, "Characterization and photocatalytic activity of Au/TiO_2 thin films for azo-dye degradation," *Journal of Catalysis*, vol. 220, no. 1, pp. 127–135, 2003.

[33] V. Subramanian, E. E. Wolf, and P. V. Kamat, "Influence of metal/metal ion concentration on the photocatalytic activity of TiO_2—Au composite nanoparticles," *Langmuir*, vol. 19, no. 2, pp. 469–474, 2003.

[34] M. Epifani, C. Giannini, L. Tapfer, and L. Vasanelli, "Sol-gel synthesis and characterization of Ag and Au nanoparticles in SiO_2, TiO_2, and ZrO_2 thin films," *Journal of the American Ceramic Society*, vol. 83, no. 10, pp. 2385–2393, 2000.

[35] M. Zhou, J. Yu, S. Liu, P. Zhai, and B. Huang, "Spray-hydrolytic synthesis of highly photoactive mesoporous anatase nanospheres for the photocatalytic degradation of toluene in air," *Applied Catalysis B*, vol. 89, no. 1-2, pp. 160–166, 2009.

[36] K. S. Sing, D. H. Everett, R. A. W. Haul et al., "Reporting physisorption data for gas/solid sysytems," *Pure and Applied Chemistry*, vol. 57, no. 4, pp. 603–619.

[37] J. Yu, W. Wang, B. Cheng, and B. L. Su, "Enhancement of photocatalytic activity of Mesporous TiO_2 powders by hydrothermal surface fluorination treatment," *Journal of Physical Chemistry C*, vol. 113, no. 16, pp. 6743–6750, 2009.

[38] J. Yu, Q. Xiang, and M. Zhou, "Preparation, characterization and visible-light-driven photocatalytic activity of Fe-doped titania nanorods and first-principles study for electronic structures," *Applied Catalysis B*, vol. 90, no. 3-4, pp. 595–602, 2009.

[39] K. I. Ishibashi, A. Fujishima, T. Watanabe, and K. Hashimoto, "Detection of active oxidative species in TiO_2 photocatalysis using the fluorescence technique," *Electrochemistry Communications*, vol. 2, no. 3, pp. 207–210, 2000.

[40] J. Yu and X. Yu, "Hydrothermal synthesis and photocatalytic activity of zinc oxide hollow spheres," *Environmental Science and Technology*, vol. 42, no. 13, pp. 4902–4907, 2008.

[41] M. Zhou, J. Yu, S. Liu, P. Zhai, and L. Jiang, "Effects of calcination temperatures on photocatalytic activity of SnO_2/TiO_2 composite films prepared by an EPD method," *Journal of Hazardous Materials*, vol. 154, no. 1–3, pp. 1141–1148, 2008.

[42] H. Takahashi, I. Harrowfield, C. MacRae, N. Wilson, and K. Tsutsumi, "Analytical TEM study on the dispersion of Au nanoparticles in Au/TiO_2 catalyst prepared under various temperatures," *Surface and Interface Analysis*, vol. 31, no. 2, pp. 73–78, 2001.

[43] T. Akita, K. Tanaka, S. Tsubota, and M. Haruta, "Analytical high-resolution TEM study of supported gold catalysts: orientation relationship between Au particles and TiO_2 supports," *Journal of Electron Microscopy*, vol. 49, no. 5, pp. 657–662, 2000.

[44] J. Yu, L. Yue, S. Liu, B. Huang, and X. Zhang, "Hydrothermal preparation and photocatalytic activity of mesoporous Au-TiO_2 nanocomposite microspheres," *Journal of Colloid and Interface Science*, vol. 334, no. 1, pp. 58–64, 2009.

[45] J. Yu, J. Xiong, B. Cheng, and S. Liu, "Fabrication and characterization of Ag-TiO_2 multiphase nanocomposite thin films with enhanced photocatalytic activity," *Applied Catalysis B*, vol. 60, no. 3-4, pp. 211–221, 2005.

[46] J. Yu, H. Tao, and B. Cheng, "In situ monitoring of heterogeneous catalytic reactions," *ChemPhysChem*, vol. 11, no. 8, pp. 1617–1618, 2010.

[47] J. Yu, G. Dai, and B. Huang, "Fabrication and characterization of visible-light-driven plasmonic photocatalyst Ag/AgCl/TiO_2 nanotube arrays," *Journal of Physical Chemistry C*, vol. 113, no. 37, pp. 16394–16401, 2009.

[48] T. Diemant, Z. Zhao, H. Rauscher, J. Bansmann, and R. J. Behm, "Interaction of CO with planar Au/TiO_2 model catalysts at elevated pressures," *Topics in Catalysis*, vol. 44, no. 1-2, pp. 83–93, 2007.

[49] A. Zwijnenburg, A. Goossens, W. G. Sloof et al., "XPS and Mössbauer characterization of Au/TiO_2 propene epoxidation catalysts," *Journal of Physical Chemistry B*, vol. 106, no. 38, pp. 9853–9862, 2002.

[50] Y. Zhang, G. Li, Y. Wu, Y. Luo, and L. Zhang, "The formation of mesoporous TiO_2 spheres via a facile chemical process," *Journal of Physical Chemistry B*, vol. 109, no. 12, pp. 5478–5481, 2005.

[51] Z. Liu, D. D. Sun, P. Guo, and J. O. Leckie, "One-step fabrication and high photocatalytic activity of porous TiO_2 hollow aggregates by using a low-temperature hydrothermal method without templates," *Chemistry*, vol. 13, no. 6, pp. 1851–1855, 2007.

[52] Q. Li, B. Guo, J. Yu et al., "Highly efficient visible-light-driven photocatalytic hydrogen production of CdS-cluster-decorated graphene nanosheets," *Journal of the American Chemical Society*, vol. 133, no. 28, pp. 10878–10884, 2011.

[53] Q. Xiang, J. Yu, and M. Jaroniec, "Enhanced photocatalytic H_2-production activity of graphene-modified titania nanosheets," *Nanoscale*, vol. 3, no. 9, pp. 3670–3678, 2011.

[54] R. K. Rana, Y. Mastai, and A. Gedanken, "Acoustic cavitation leading to the morphosynthesis of mesoporous silica vesicles," *Advanced Materials*, vol. 14, no. 19, pp. 1414–1418, 2002.

[55] P. Madhusudan, J. Ran, J. Zhang, J. Yu, and G. Liu, "Novel urea assisted hydrothermal synthesis of hierarchical $BiVO_4$/$Bi_2O_2CO_3$ nanocomposites with enhanced visible-light photocatalytic activity," *Applied Catalysis B*, vol. 110, pp. 286–295, 2011.

[56] J. Yu, L. Zhang, B. Cheng, and Y. Su, "Hydrothermal preparation and photocatalytic activity of hierarchically sponge-like macro-/mesoporous Titania," *Journal of Physical Chemistry C*, vol. 111, no. 28, pp. 10582–10589, 2007.

[57] Q. Xiang, J. Yu, and M. Jaroniec, "Nitrogen and sulfur co-doped TiO_2 nanosheets with exposed 001 facets: synthesis, characterization and visible-light photocatalytic activity," *Physical Chemistry Chemical Physics*, vol. 13, no. 11, pp. 4853–4861, 2011.

[58] H. Fu, C. Pan, W. Yao, and Y. Zhu, "Visible-light-induced degradation of rhodamine B by nanosized Bi_2WO_6," *Journal of Physical Chemistry B*, vol. 109, no. 47, pp. 22432–22439, 2005.